CFC7 **9:30 am**

Reliability studies of wafer-bonded InGaAs P-I-N photodetectors on GaAs substrates

F. E. Ejeckam, C. L. Chua, Z.-H. Zhu, Y. H. Lo, M. Hong,* J. P. Mannaerts,* R. Bhat,**
School of Electrical Engineering, Cornell University, Ithaca, New York 14853

We present the first reliability studies of InGaAs P-I-N photodiodes wafer-bonded to GaAs substrates. The P-I-N photodiodes used for our reliability studies have shown record low dark currents (< 100 pA for about 40% of the devices) and a high responsivity of 1 A/W at 1.55-μm wavelength. The detailed characteristics of the P-I-N detectors wafer-bonded to both GaAs and Si have been published elsewhere.[1] The focus of this paper will be on the degradation of the devices under high temperature operation (60°C) and thermal cycling (23 to 95°C).

The capability of integrating two lattice-mismatched material systems is important for optoelectronic integration and innovative photonic device fabrication. The wafer-bonding process[2,3] has been very successful in many device demonstrations. In making the wafer-bonding process a viable technology for commercial device manufacturing, reliability becomes a pressing issue. Because the dark current of a P-I-N photodetector is known to be most sensitive to material and process-induced defects, we monitored and report the change in dark currents (due to high-temperature operation and thermal cycling) as the indicator for device degradation.

Figure 1 shows a schematic and SEM photograph of the InGaAs detectors bonded to a GaAs substrate. The devices had an etched mesa structure and an AR-coated photosensitive area of about 6400 μm.[2] The circular top metal contact is shown in the pictures and the bottom contact is on the back of the GaAs substrate. Thus, the photocurrent has to pass the InP/GaAs bonding interface. The resistance at the bonding interface was found to be lower than 17 Ω from the forward bias I-V measurement of the photodiode.

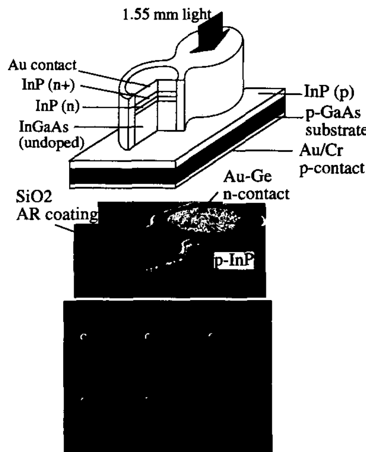

CFC7 **Fig. 1** Schematic and SEM photograph of an array of wafer-bonded InGaAs P-I-N detectors.

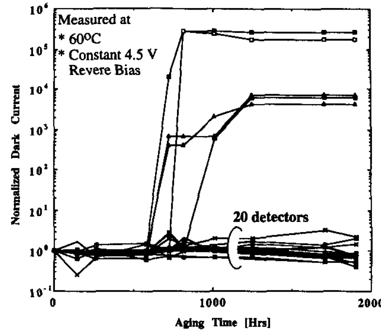

CFC7 **Fig. 2** Normalized dark currents measured under constant 4.5 V reverse bias at 60°C.

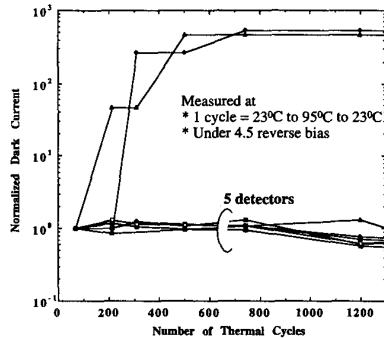

CFC7 **Fig. 3** Normalized dark currents measured under constant 4.5 V reverse biasing and thermal cycling.

In the device aging test, an array of photodetectors were reverse-biased at 4.5 V continuously for over 1900 h at 60°C. All the devices had an initial dark curent of less than 5 nA, and all except a few devices had their dark current around or lower than 1 nA. Figure 2 shows the results of the aging test. Twenty of the 25 devices that were measured showed no measurable increase in their dark current. In a separate experiment, an array of photodiodes reverse-biased at 4.5 V were subject to temperature cycles from 23°C to 95°C to 23°C for over 1300 times. Each thermal cycle took about 30 min and was done with a power controlled IR lamp. Figure 3 shows the change of the device dark currents after thermal cycles. Five of the 7 devices measured retained their original dark currents. In both experiments, then almost all of the devices showed no degradation, indicating that the wafer bonding process does not seem to affect the device reliability. We suspected that the failures for these few devices were due to electro statics and packaging, extrinsic instead of intrinsic reasons.

**AT&T Bell Laboratories, 600 Mountain Avenue, Murray Hill, New Jersey 07974*
***Bellcore, 331 Newman Springs Road, Red Bank, New Jersey 07701*

1. F. E. Ejeckam, C. L. Chua, Z.-H. Zhu, Y. H. Lo, M. Hong, R. Bhat, Appl. Phys. Lett. (1995).
2. Y. H. Lo, R. Bhat, D. M. Hwang, M. A. Koza, T. P. Lee, Appl. Phys. Lett. 58, 1961 (1991).
3. Z. L. Liau, D. E. Mull, Appl. Phys. Lett. 56, 737 (1990).

CFC8 **9:45 am**

Epitaxial lift-off for wafer-scale GaAs-on-Si semi-monolithic integration

Wei Chang, Mark Goertemiller, Ashish Verma, Eli Yablonovitch, *UCLA, Electrical Engineering Department, Los Angeles, California 90095-1594*

The use of GaAs components (e.g. LEDs and photodiodes) onto Si circuitry has unveiled new opportunities in optoelectronic systems packaging. Current techniques, like flip-chip bonding[1] and thin film grafting,[2,3] have demonstrated GaAs photonic devices integrated onto Si VLSI. The epitaxial lift-off (ELO) technique is quite promising, but needs to be improved for wafer-scale integration. Herein we report a potential manufacturable ELO process that allows wafer-scale GaAs-on-Si integration. An epi-layer from 2″ GaAs wafer, containing LEDs and photodiodes, are lifted-off and bonded onto a 5″ processed Si wafer containing functional circuits. The integrated module can be used for optical interconnect technology.

The desired lift-off pattern is first defined on a GaAs wafer with 10-μm-thick photoresist. After hard baking, photoresist can be made more than 10-μm thick, which allows etching channels to permit dilute hydrofluoric (HF) acid to penetrate under the GaAs epi-layer and uniformly lift-off all the devices. Actually, before the HF etching step, the GaAs wafer is bonded to a sapphire disk for mechanical support during lift-off and transfer. Figure 1 shows an array of LEDs epitaxially lifted-off and attached onto a sapphire carrier. Illustrated in Fig. 2 is an SEM photograph that displays the topography of LED thin films attached to a sapphire disk after ELO. After the ELO process, GaAs epi-layer thin films, which are now carried on a sapphire disk, are transferred and bonded onto Si wafers. The

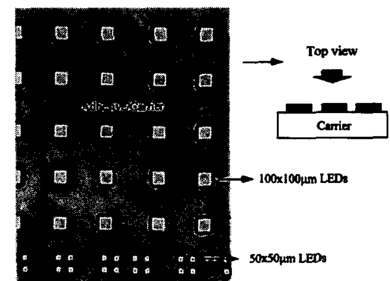

CFC8 **Fig. 1** An array of LEDs are epitaxially lifted-off and attached onto a transparent sapphire carrier.

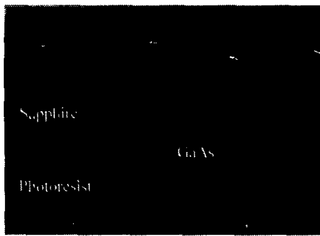

CFC8 Fig. 2 SEM photograph of ELO LEDs thin films on sapphire disk.

use of a transparent sapphire carrier allows precise alignment of GaAs devices onto Si wafers. The details of this integration process, the thin-film bonding technique, the alignment accuracy, and the performance of LEDs and photodiodes on Si for optical interconnects are presented.

In conclusion, we have developed a manufacturable epitaxial lift-off process to integrate a 2" GaAs epi-layer containing active photonic devices onto a much larger 5" processed Si VLSI wafer. The availability of this ELO hetero-integration process will be extremely valuable in high-performance and reliable optoelectronic integrated systems.

1. K. W. Goossen, J. A. Walker, *et al.*, IEEE Photon. Technol. Lett. **7**, 360 (1995).
2. C. Camperi-Ginestet, M. Hargis, N. Jokerst, M. Allen, IEEE Photon. Technol. Lett. **3**, 1123 (1991).
3. E. Yablonovitch, T. J. Gmitter, J. P. Harbison, R. Bhat, Appl. Phys. Lett. **51**, 2222 (1987).

CFD — 8:00 am, Room B4

Ultrafast Fiber Lasers I

Steven A. Newton, *Hewlett-Packard, Presider*

CFD1 — 8:00 am

Cladding-pumped passively mode-locked femtosecond fiber lasers

M. E. Fermann, D. Harter, J. D. Minelly,* G. G. Vienne,* *IMRA America, Inc., 1044 Woodridge Ave., Ann Arbor, Michigan 48105*

Many currently pursued applications of femtosecond erbium fiber lasers would greatly benefit from the availability of higher pulse energies and higher pulse repetition rates than presently available from compact oscillator designs. However, though erbium oscillator designs have been developed that allow the generation of femtosecond pulses with energies in excess of 1 nJ and passive harmonic mode-locking has allowed the extension of achievable repetition rates into the GHz regime, the distribution of such lasers has been limited because they relied on the use of expensive high-power pump lasers such as MOPAs[1] or Ti:sapphire lasers.[2]

Here we demonstrate for the first time that high-power and high-repetition-rate femtosecond fiber lasers can be constructed that require only simple broad-area diode-array pump lasers. To allow pumping with diode arrays, the standard single-mode erbium fiber of conventional oscillator designs is replaced with double-clad erbium/ytterbium fiber. Reliable femtosecond pulse operation is ensured by exploiting nonlinear polarization evolution for steady-state pulse shaping in an environmentally stable cavity.[3] Furthermore the use of chirped Bragg gratings[4] allows the extension of the operation range of these types of laser into the picosecond regime.

The experimental setup for a cladding-pumped passively mode-locked fiber oscillator is shown in Fig. 1. As the gain medium we used a single 2–4 m length of Er^{3+}/Yb^{3+} doped fiber to allow pumping of Er^{3+} via energy transfer from Yb^{3+}. Additional lengths of standard telecom or dispersion-compensating (non-soliton supporting) fiber could also be spliced into the cavity, giving fundamental cavity repetition rates between 8 and 30 MHz.

The active fiber was pumped through a dichroic mirror with a standard 1 W, 100 × 1 μm broad-area diode array operating at 976 nm. Even with an active fiber length as short as 2.0 m a cw output power up to 40 mW could be achieved.

For pulse start up and to enable soliton repulsion in the cavity, we employed semiconductor saturable absorbers with a range of different life-times. A minimum pulse width of around 170 fsec (bandwidth-limited) was generated, limited by the relatively narrow bandwidth of the Er/Yb fiber. A typical autocorrelation and the corresponding pulse spectrum of a 200 fsec pulse are shown in Fig. 2. At a fundamental repetition rate of 30 Mhz a mode-locked output power up to 3 mW was obtainable, whereas passive harmonic mode-locking at 200 MHz produced an output power of ≈10 mW. The number of pulses (for a fundamental repetition rate of 8.33 MHz) in the cavity measured when ramping the pump-current up and down is shown in Fig. 3. In this a pump current of 1400 mA corresponds to a launched pump power of ≈500 mW. A significant amount of hysteresis is observed between up and down-ramping of the pump power. In down-ramping the number of pulses drops reliably one by one. This indicates a well-defined stability range for each repetition rate in the laser.

Due to the small residual pulse jitter in passive harmonically mode-locked lasers, sidebands in the RF-spectrum show up at the fundamental cavity frequency. We were able to obtain a sideband suppression of > = 70 dB, with an estimated corresponding pulse jitter of less than 10 psec.

Finally, we were also able to operate the lasers in the psec regime by adding a chirped fiber Bragg grating to the cavity.

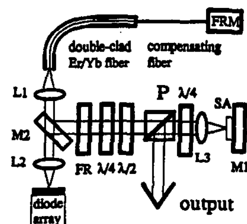

CFD1 Fig. 1 Setup of a harmonically mode-locked cladding-pumped fiber laser. FR = Faraday rotator, P = polarizer.

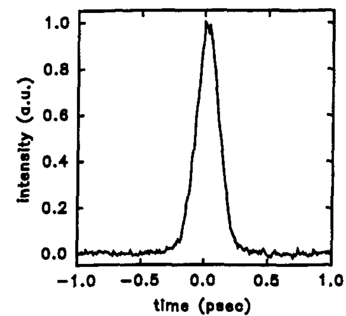

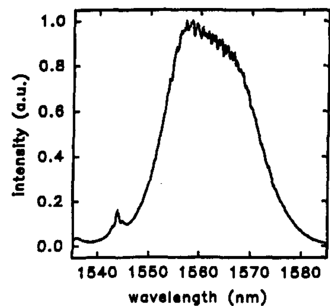

CFD1 Fig. 2 Typical autocorrelation and pulse spectrum of a generated 200 fsec pulse.

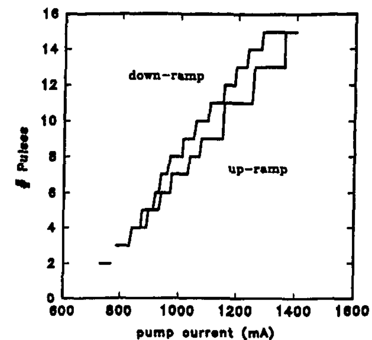

CFD1 Fig. 3 Number of pulses in cavity for a fundamental repetition rate of 8.33 MHz as a function of slow up- and down-ramping of the pump current.